

Low-temperature resistivity of ordered and disordered $A15$ compounds

M. Gurvitch,* A. K. Ghosh, H. Lutz,[†] and M. Strongin

Brookhaven National Laboratory, Upton, New York 11973

(Received 8 October 1979)

The low-temperature electrical resistivity has been measured for the high- T_c $A15$ compounds Nb_3Sn , Nb_3Al , and Nb_3Ge and also a low- T_c compound Mo_3Ge . It is found that most of the high- T_c $A15$'s exhibit a T^2 dependence in the temperature range $T_c < T \leq 40$ K, while Mo_3Ge shows a T^5 dependence on temperature. Data are also presented for irradiated Nb_3Sn which show that the T^2 power law is preserved for increasing residual resistivity $\rho(0)$. Previous analyses of $A15$ resistivity are examined in some detail to show that the T^2 dependence in the low-temperature resistivity of high- T_c $A15$ materials is an intrinsic effect and is not crucially dependent on the real phonon structure in these materials. It is argued that the observed T^2 dependence remains an unsolved theoretical problem.

I. INTRODUCTION

The normal-state electrical resistivity $\rho(T)$ of high- T_c $A15$ compounds such as Nb_3Sn , Nb_3Al , Nb_3Ge , V_3Si , etc., differs significantly from that of a typical metal at both low and high temperatures. In this paper we shall concentrate on the low-temperature ($T_c < T \leq 50$ K) behavior of $A15$'s with emphasis on Nb_3Sn . Some of the results in the regime where $T \geq 50$ K have already been published,^{1,2} and more complete results will be published separately.

In the past, two functional forms for $\rho(T)$ at low temperatures have been proposed to describe the resistivity behavior of $A15$ compounds. Initially, Woodard and Cody³ found empirically that the $\rho(T)$ of single crystal Nb_3Sn could be expressed over a range of temperature $T_c < T < 850$ K as

$$\rho(T) = \rho(0) + bT + d \exp(-T_0/T) \quad (1)$$

b , d , and T_0 are constants and $\rho(0)$ is an extrapolation of the resistivity to zero temperature. The exponential term described the rapid increase in $\rho(T)$ at low T as well as the negative curvature at high T . For Nb_3Sn T_0 was found to be ~ 85 K. Subsequently Williamson and Milewits⁴ reported that for Nb_3Sn the $\rho(T)$ could be fitted by using Eq. (1) with $b = 0$ in the range $T < 100$ K. They argued that the exponential term was due either to phonon assisted interband scattering or to intraband umklapp scattering.

For Nb_3Sn and also for Nb_3Al and Nb_3Ge another low-temperature characterization was proposed by Webb *et al.*⁵ They found that below 50 K, these high- T_c $A15$ compounds have resistivities which vary closely as T^2

$$\rho(T) = \rho(0) + AT^2 \quad (2)$$

They interpreted this low-temperature behavior as

arising from a Wilson-type s - d electron-phonon scattering model⁶ with a non-Debye phonon spectrum which changed the temperature dependence from the usual T^3 behavior to a T^2 behavior. For V_3Si , the resistivity was also found to vary as T^2 in the range $T \leq 29$. Marchenko⁷ who first observed this behavior in V_3Si attributed the T^2 behavior to electron-electron scattering mechanism.

In this paper precision measurements of the resistivity of some $A15$ compounds in the range $T_c < T \leq 40$ K are reported. The resistivity data were analyzed using a simple method which is discussed in detail in the Appendix. The results of these analyses suggest the following: (a) The functional dependence of $\rho(T)$ for Nb_3Sn , Nb_3Al , and Mo_3Ge does not seem to be of the exponential form. Rather, $\rho(T)$ seems to have a power-law dependence with the power index n equal to 2 for the high- T_c Nb_3Sn and Nb_3Al , and equal to 5 for the low- T_c Mo_3Ge samples. (b) It was also found that as the residual resistivity $\rho(0)$ of Nb_3Sn was increased by radiation damage, $\rho(T)$ still seemed to have a T^2 dependence.

The various physical mechanisms that have been proposed to explain the low-temperature behavior of $\rho(T)$ for $A15$ compounds are examined. It is argued that mechanisms like the electron-electron scattering⁷ and the electron-phonon interband scattering with non-Debye-like phonon structure⁵ are inadequate to explain all the data. Finally, an interesting link between the saturation model² proposed to explain the high-temperature resistivity data of these materials and the behavior of the coefficient A as a function of disorder is discussed.

II. EXPERIMENTAL TECHNIQUES

Polycrystalline samples of $A15$ materials of nominal thickness 0.2–1.0 μm were synthesized by elec-

tron beam coevaporation of elements in ultra-high vacuum $< 10^{-7}$ torr. The material was deposited on polished single-crystal sapphire substrates which were heated to 750–900°C. The compositions of the samples were analyzed using microprobe techniques. All samples used for resistivity measurements were chosen to be close to the ideal $A15$ composition. Samples were also checked by x-ray diffractometer techniques to ensure that they were ordered single phase $A15$ structure. The exact degree of order was not obtained for the samples owing to preferred orientation, however, to the limits of detectability no second phase was observed. Sample thickness was measured by a Sloan Dektak surface profile measuring system.

The substrates were masked during evaporation to provide a comblike geometry with "fingers" being connected to the long "spine." The "fingers" were mechanically etched to provide "point" contact along the "spine." This technique allowed the measurement of absolute resistivity to a precision of $\pm 5\%$. Details of this technique can be found in Ref. 8.

The resistivity of the samples was measured by a standard four-probe technique using a calibrated germanium thermometer to monitor the temperature from 1.5 to 55 K. The sample current used was of the order of 3–4 mA. All voltage readings were monitored by a multichannel millivoltmeter DORIC-220. The "DORIC" was interfaced with a Tektronix-4051 computer which read data from the DORIC and stored it on magnetic tape for analysis. Sample voltage measurements were usually taken at 0.1 K intervals.

To study the resistivity behavior of $A15$ compounds in different states of disorder, we chose Nb_3Sn primarily because of its ease in synthesizing clean samples with $\rho(0) \sim 10\text{--}15 \mu\Omega \text{ cm}$. The $\rho(0)$ of Nb_3Sn samples were increased by either 2.0-MeV electron irradiation at the Brookhaven Dynamitron or by 2.5-MeV α particles in the Brookhaven "small" Van de Graaff. To assure uniform irradiation the beam was rastered in the X and Y directions using magnetic coils on the beam pipe. The electron irradiations presented us with a severe heating problem. Electrons have a very small scattering cross section and in order to achieve significant damage in a sample, doses of the order of $10^{19}\text{--}10^{20}$ electrons/ cm^2 were required, as compared to doses of $\sim 10^{16}\text{--}10^{17}$ α part./ cm^2 . To obtain these high electron doses in a reasonable time, beam currents of 50 to 200 μA over an area of $\sim 0.5\text{--}0.7 \text{ cm}^2$ were used which resulted in a power dissipation on the target of the ~ 200 to 800 W/cm^2 . However, with a steady flow of water through the copper pipe on the back of the holder the sample temperature was held below 50°C during the irradiation. The latter was achieved by using a thin layer of Ga between the sapphire and the copper block. Since the resistance of Nb_3Sn is fairly sensi-

tive to changes in temperature at about 300 K, the temperature rise of the sample was estimated by monitoring the sample resistance during the initial stages of irradiation.

III. EXPERIMENTAL RESULTS

The resistivity data for the $A15$ materials studied were analyzed by the deviation-plot method (DP) which is discussed in the Appendix. We briefly state here that in this plot the best fit is given by the dependence for which $\Delta\rho \sim 0$. In Figs. 1(a) and 1(b) the DP of Nb_3Sn [$\rho(0) = 11.4 \mu\Omega \text{ cm}$] is shown in the temperature range $T_c < T < 30 \text{ K}$, clearly indicating that n , the power index, is equal to 2 ± 0.1 . Similarly Nb_3Al [$\rho(0) \sim 54 \mu\Omega \text{ cm}$] also shows a T^2 dependence. In the case of Nb_3Ge only one sample with a $\rho(0) \sim 50 \mu\Omega \text{ cm}$ was analyzed and was found to have the best fit for $n = 2.3$. Perhaps the noninteger n may have something to do with the inevitable presence of a second phase in Nb_3Ge .⁹ Data for single crystal V_3Si ($\rho_0 \sim 4 \mu\Omega \text{ cm}$) were also analyzed by the DP method and showed a T^2 dependence to $\sim 26\text{--}28 \text{ K}$. (Data for single crystal V_3Si were kindly provided by R. Caton.) However, the low- T_c $A15$ compound Mo_3Ge with a $\rho(0) \sim 0.2 \mu\Omega \text{ cm}$ turned out to have a $n = 5$,¹ behaving as if it were a good Bloch-Grüneisen metal, which is expected for a low d -band density-of-states material. In Table I is listed the index n for the different $A15$'s and the range of T over which a very good fit is obtained. Beyond these specified temperature ranges, the n start to deviate from their integer values. In all cases except V_3Si , n tends to decrease if a wider temperature range is chosen. Deviation of n towards the smaller values is expected if the resistivity is governed by a behavior analogous to the classical Bloch-Grüneisen or Wilson formulas.⁶ n would also decrease from the viewpoint of saturation^{10,11} in the resistivity when the $\rho(T)$ curve starts to deviate towards the T axis. For $T = 40 \text{ K}$, the data for Nb_3Sn deviates from the T^2 fit by $\sim 1\%$.

The behavior of the resistivity of disordered high- T_c $A15$'s was studied by irradiating Nb_3Sn samples. In Fig. 2 is shown the general trend in the data as the Nb_3Sn sample 2 is successively electron irradiated. A DP analysis of these data show that n stays equal to 2 with increasing $\rho(0)$. A similar result (Fig. 3) was found for an α -irradiated Nb_3Sn sample 1 with $\rho(0) = 75.7$ and $95.7 \mu\Omega \text{ cm}$. [The plots for the same unirradiated sample with $\rho(0) = 11.4 \mu\Omega \text{ cm}$ are shown in Fig. 1(a).] Deviation plots for all the intermediate irradiations also give $n = 2$. We see that in all cases, even when $\rho(0)$ is as high as $96 \mu\Omega \text{ cm}$, the resistivity $\rho(T) - \rho(0)$ remains proportional to T^2 . It should be mentioned that even in the highly irradiated state, the Nb_3Sn retains its $A15$ structure

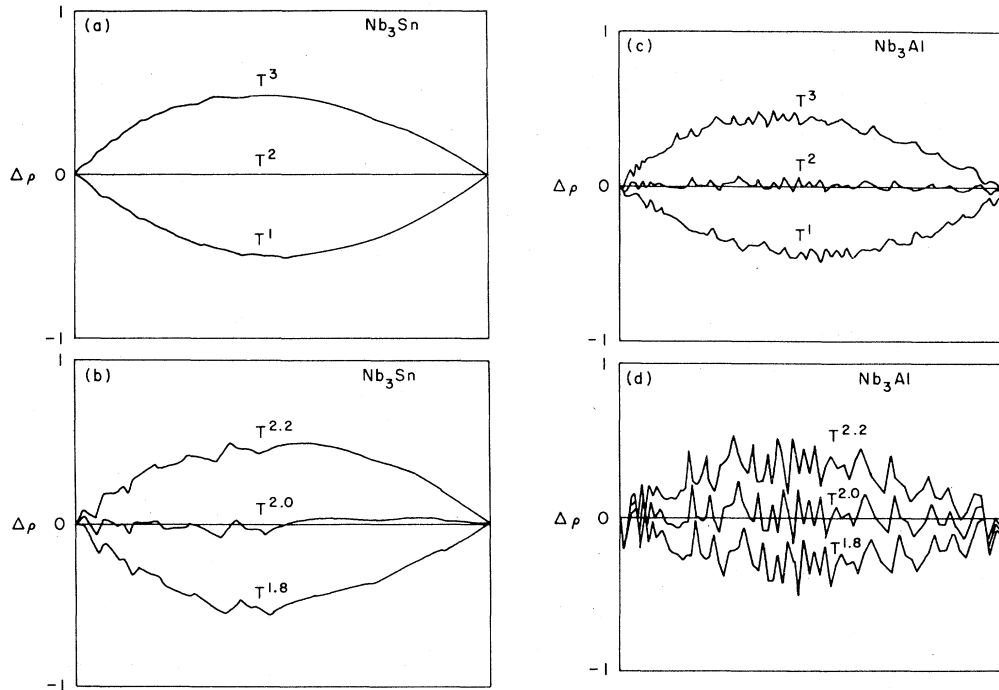


FIG. 1. Low-temperature data presented as deviation plots. Data points are connected by straight lines. (a) "As-deposited" Nb_3Sn , $\rho(0) = 11.4 \mu\Omega \text{ cm}$, $18.4 \leq T \leq 28.1 \text{ K}$; (b) same as (a) with $\Delta\rho$ increased by a factor of 10; (c) "as-deposited" Nb_3Al , $\rho(0) = 53.8 \mu\Omega \text{ cm}$, $18.6 < T \leq 35.8 \text{ K}$; (d) same as (c) except $\Delta\rho$ increased by a factor of 5.

although the lattice is larger due to the radiation induced disorder.

An interesting feature of the data is that the " T^2 law" extends to higher temperatures in the damaged samples. In the clean, unirradiated samples of Nb_3Sn , the " T^2 law" holds to $T_2 \sim 28\text{--}30 \text{ K}$. Increasing the temperature above that limit would lead, in a clean sample, to distortions of the deviation plot and to the decrease of n from 2 to lower values. However, with disorder T_2 definitely increases: $T_2 \approx 37 \text{ K}$ for $\rho(0) \approx 62 \mu\Omega \text{ cm}$ and $T_2 \approx 44 \text{ K}$ for $\rho(0) \approx 96 \mu\Omega \text{ cm}$. The errors on the T_2 values are of the order of a few degrees. Figure 4 summarizes the results obtained for Nb_3Sn and other $A15$'s. In-

TABLE I. Power-law index for $A15$ compounds.

Material	Index n	Temperature range (K)
Nb_3Sn	2.0 ± 0.05	$T_c < T < (28\text{--}30)$
Nb_3Al	2.0 ± 0.05	$T_c < T < (35\text{--}40)$
V_3Si^a	2.0 ± 0.2	$T_c < T < (26\text{--}28)$
Nb_3Ge	2.3 ± 0.2	$T_c < T < (\sim 35)$
Mo_3Ge	5.0 ± 0.1	$10 < T < (\sim 35)$

^a Single-crystal data kindly provided by R. Caton.

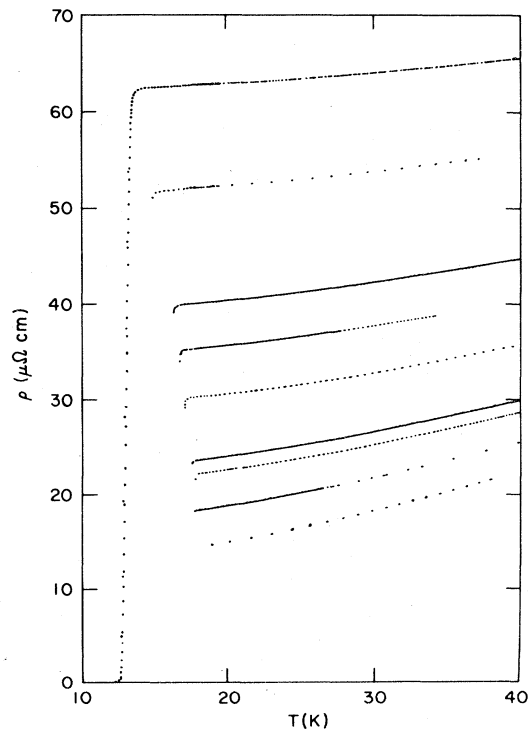


FIG. 2. Low-temperature resistivity data for electron irradiated Nb_3Sn , No. 2.

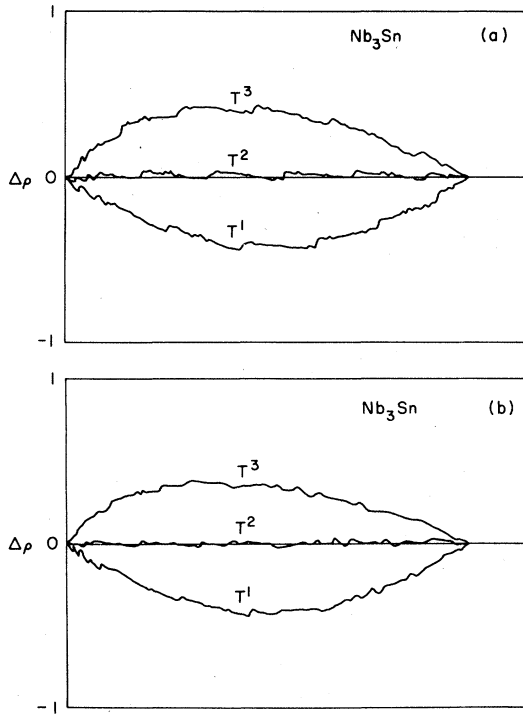


FIG. 3. Deviation plots for α -irradiated Nb_3Sn . (a) $\rho(0) = 75.7 \mu\Omega \text{ cm}$, $16.3 < T < 33.4 \text{ K}$; (b) $\rho(0) = 95.7 \mu\Omega \text{ cm}$, $14.9 < T < 43.6 \text{ K}$.

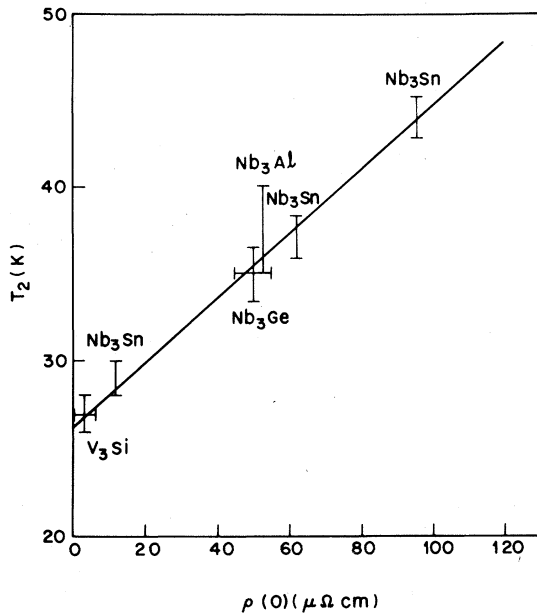


FIG. 4. Dependence of the upper limit in temperature T_2 to which resistivity is proportional to T^2 on the residual resistivity $\rho(0)$ for different A15's. Nb_3Sn sample was α -irradiated.

Interestingly enough, all the samples fall on one straight-line plot.

With increasing $\rho(0)$, the coefficient A in the expression for the resistivity $\rho(T) = \rho(0) + AT^2$ decreases, as can be seen from Fig. 5 where A is plotted as a function of $\rho(0)$ for three Nb_3Sn samples (see Table II for A values). This graph shows that for a given material, A can be considered to be a function of $\rho(0)$. Note the several dots indicated by the arrow near the upper part of the graph. These dots (7 in all, although this is not evident from the graph) represent the scatter in the measurements of the coefficient A of the reference (unirradiated) part of the electron-irradiated sample 2. The reference part of the sample was masked during the irradiations [actually it still received a small dose as can be seen from the small $\rho(0)$ change in Table II], and it was measured each time along with the irradiated part. The space occupied by these dots gives some idea of the precision in the determination of A , or about the size of the error bars for a set of A values corresponding to a single sample. The shift along the $\rho(0)$ axis between the data for different samples is most likely due to the error in the determination of the geometrical factor for the resistivity.

In concluding this section we mention that for the low- T_c A15 compound Mo_3Ge , the T^5 behavior is observed for $\rho(0)$ as high as $30 \mu\Omega \text{ cm}$.¹ For this $\rho(0)$, it has as $T_c \sim 2.6 \text{ K}$ and a value of λ , the

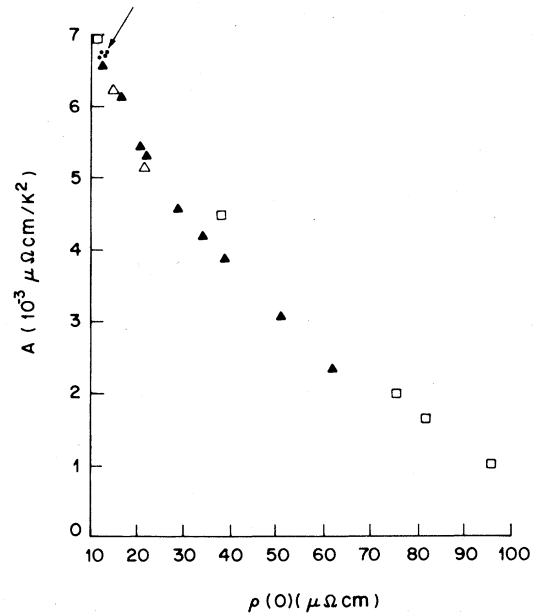


FIG. 5. A vs $\rho(0)$ for three Nb_3Sn samples: \square : α -irradiated sample 1; Δ : α -irradiated sample 3; \blacktriangle : electron-irradiated sample 2.

TABLE II. Coefficient A for irradiated Nb₃Sn samples.

Sample	$\rho(0)$ ($\mu\Omega$ cm)	A ($10^3 \mu\Omega$ cm/K ²)	$\rho(0)$ Reference	A (10^3) Reference
1	11.4	6.974		
1	37.95	4.482		
1	75.69	1.982		
1	82.03	1.63		
1	95.73	0.997		
2	12.43	6.55	14.55	6.367
2	16.408	6.103	14.65	6.409
2	20.594	5.418	14.77	6.367
2	21.998	5.28	14.75	6.391
2	28.843	4.544	15.0	6.315
2	34.068	4.168	15.4	6.33
2	38.908	3.857	15.6	6.323
2	51.15	3.046		
2	62.038	2.317		
3	14.8	6.22	13.2	6.8
3	21.4	5.15	13.3	6.83

electron-phonon coupling parameter of 0.43, estimated from McMillan's equation¹¹ with $\mu^* = 0.1$ and $\Theta_D = 435$ K. However, for the most disordered Nb₃Sn for which n was measured [$\rho(0) = 96 \mu\Omega$ cm, $T_c = 9.1$ K], the parameter λ changed from an initial value of ~ 1.8 (in the unirradiated state) to approximately 1. This observation suggests that the T^2 behavior is likely to be seen in high- λ systems. However it is not directly related to the electron-phonon coupling parameter which occurs in superconductivity.

IV. DISCUSSION

In this section we first examine previous analyses of the $A15$ resistivity, in particular the exponential fits⁴ and the interband scattering model with non-Debye-like phonon structure proposed by Webb and co-workers⁵; secondly, an interesting connection between the saturation model and the behavior of the coefficient A with disorder is shown; and finally, other physical mechanisms which can give rise to a low-temperature T^2 dependence in the resistivity are briefly discussed.

A. Previous analyses of $A15$ resistivity data

Williamson and Milewits⁴ showed that for $T < 100$ K the resistivity data of single crystal Nb₃Sn could be described very well by an expression of the form

$$\rho(T) = \rho(0) + d \exp(-T_0/T)$$

The exponential term was explained on the basis of either phonon-assisted interband or to intraband umklapp scattering. To test the exponential dependence we have used the DP method to analyze our data on Nb₃Sn in the unirradiated state. This was done by using the variable $x = \exp(-T_0/T)$ and scanning different values of T_0 in the same way as was done with values of z (see Appendix). Deviation plots obtained in this way for unirradiated Nb₃Sn sample 1 showed that in the temperature range $18.3 < T < 40.3$ K, the data deviated systematically from the exponential fit for T_0 in the range 70–90 K. Even for a smaller temperature range $18.3 < T < 28.2$ K, the exponential term did not seem to be the correct functional dependence on temperature. We also tried to include a linear term, bt , but did not succeed in improving the fit. Based on our analyses we must conclude that the exponential term does not represent the correct functional dependence for $T < 40$ K, at least in the case of Nb₃Sn.

From our analysis of the data, we find that the T^2 term provides the correct functional dependence of $\rho(T)$ for $T < 40$ K. To explain similar behavior Webb *et al.*⁵ argued that the T^2 dependence was essentially a coincidence owing to the non-Debye-like phonon structure $F(\omega)$. It is important to distinguish whether this mechanism or a more intrinsic mechanism is needed to explain the T^2 behavior. Their idea is that the phonon density of states $F(\omega)$ of the high- T_c $A15$ compounds differs from the Debye approximation where $F(\omega) \propto \omega^2$, in such a way as to reduce the power index $n = 3$, which occurs in Wilson's model,⁶ to the observed value of $n = 2$.

The use of a realistic $F(\omega)$ may very well reduce n from 3 to some lower value; however, we argue that there are two factors that make it implausible. First, if the observed value of n is due to the peculiarities of a phonon spectrum, then it is hard to understand why n is an integer, and in more than one material. Secondly, if the explanation is correct, then n should change as the phonon spectrum is altered. However, even in highly disordered Nb_3Sn samples with $\rho(0) \sim 96 \mu\Omega \text{ cm}$ where the phonon frequencies would be expected to change, n remains the same. A more detailed discussion of this explanation can be found in Ref. 12.

B. Saturation and the behavior of A

In this section is discussed a link between the saturation model² and the behavior of the coefficient A with disorder. In the parallel resistor model, resistivity is considered to behave as $\rho^{-1}(T) = \rho_{\text{id}}^{-1}(T) + \rho_{\text{max}}^{-1}$ where $\rho_{\text{id}}(T)$ is the "ideal" resistivity, i.e., the resistivity that the material would have in the absence of saturation. The latter is represented by a constant "shunting" resistivity ρ_{max} which serves as a maximum value of the resistivity corresponding roughly to scattering with a mean free path of the order of an interatomic distance.

In Fig. 5 it is seen that A is a rapidly decreasing function of $\rho(0)$. One very simple way to understand this behavior is to assume that the resistivity curve is being "squeezed" between the $\rho(0)$ and ρ_{max} values. In other words, $\rho(T)$ becomes flatter as $\rho(0)$ increases because of the shunting effect of ρ_{max} , while $\rho_{\text{id}}(T)$ obeys Matthiessen's rule. It turns out that the temperature dependence of the $\rho_{\text{id}}(T)$ has the same functional form $\rho_{\text{id}}(T) = \rho_{\text{id}}(0) + A_{\text{id}}T^2$ as the measured resistivity $\rho(T)$ for $\rho(0)/\rho_{\text{max}} \leq \frac{2}{3}$; [this was checked with the deviation plots for $\rho_{\text{id}}(T)$]. The coefficient A_{id} can be found for the ideal branch in the same way the coefficient A was found for the $\rho(T)$.

We can further ask what value of ρ_{max} is needed to explain the observed behavior of the coefficient A with disorder, or, equivalently what value of ρ_{max} is needed to keep coefficient A_{id} constant. In Fig. 6 the standard deviation δ of the coefficient A_{id} for the series of irradiations is plotted versus ρ_{max} values. The best ρ_{max} is obviously the one which minimizes δ . We see that for the two Nb_3Sn samples (one irradiated with α particles and the other with electrons) the best values of ρ_{max} are ~ 145 and $\sim 135 \mu\Omega \text{ cm}$, respectively. For the Mo_3Ge sample the best ρ_{max} is $\sim 110 \mu\Omega \text{ cm}$.

It is remarkable that values of ρ_{max} obtained in this way (with no relation whatsoever to the behavior of the resistivity curve at high temperature) are very close to the average value of ρ_{max} used in the high-temperature fits.^{1,2,8} Even the difference in ρ_{max}

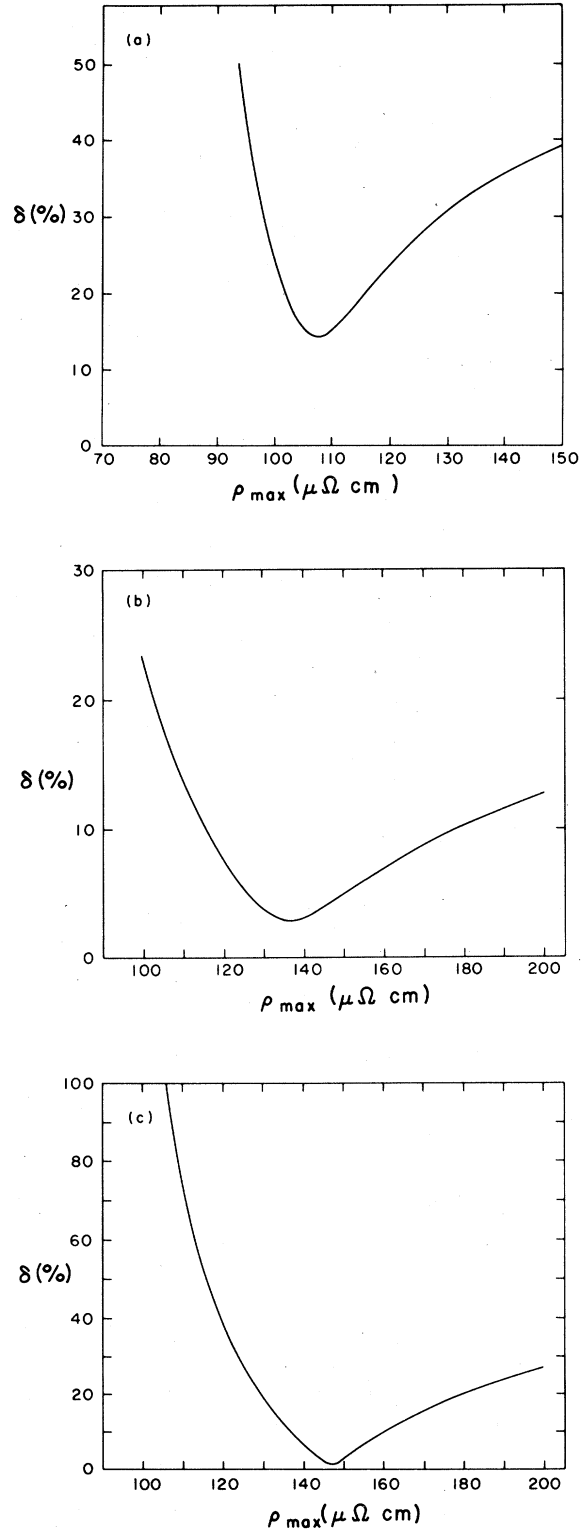


FIG. 6. Standard deviations of A_{id} values vs ρ_{max} . (a) Electron-irradiated Nb_3Sn No. 2; (b) α -irradiated Nb_3Sn No. 1; (c) α -irradiated Mo_3Ge .

between Nb₃Sn and Mo₃Ge found in the high-temperature fits appear to be reflected here. This result is viewed as another confirmation of the phenomenological parallel resistor formula and of the idea of saturation in general.

The increase of T_2 with $\rho(0)$ (Fig. 4) can also be attributed to the "parallel resistor" model. Indeed, application of the DP method to the ideal branch shows that $\rho_{\text{id}}(T) - \rho(0)_{\text{id}} = A_{\text{id}}T^2$ within a temperature range $T_c < T < T_2^{\text{id}}$, where T_2^{id} is roughly independent of $\rho(0)$ or $\rho(0)_{\text{id}}$. For Nb₃Sn, $T_2^{\text{id}} \approx 35 \pm 3$ K. From this point of view the straight-line plot of Fig. 6 means that as $\rho(0)$ increases, the curves become flatter and the T_2 region widens because of the "shunt resistor" ρ_{max} .

C. Various theoretical explanations for T^2 behavior

The T^2 behavior is seen not only in the high- T_c A15's but also has been observed in amorphous and disordered alloys.¹³ There has been theoretical work by Gubanov,¹⁴ Cote and Meisel,¹⁵ and Ohkawa¹⁶ where a T^2 dependence has been predicted for amorphous and disordered metals at low temperatures. In particular, Gubanov showed that in a lattice with *no* long-range order electrons can be scattered by phonons without obeying the law of conservation of momentum within the electron-phonon system. This mechanism can produce an asymptotic T^2 dependence at low temperatures; however, it does not apply to crystalline materials such as the A15's where long-range order *is* observed.

Another mechanism for a T^2 behavior is electron-electron scattering, in which case the coefficient $A \propto [N_{\text{bs}}(0)]$,^{7,17} where N_{bs} is the band-structure electronic density of states at the Fermi energy. However, as was noted in Ref. 5, the magnitude of A in the clean A15's is two orders of magnitude higher than in the transition metals. For example, $A_{\text{Pd}} = 3.5 \times 10^{-5} \mu\Omega \text{ cm K}^{-2}$, while $A_{\text{Nb}_3\text{Sn}} = 6.5 \times 10^{-3} \mu\Omega \text{ cm K}^{-2}$ (see Table II). This difference cannot be accounted for by the known specific-heat coefficients γ , for these two materials. For example, $\gamma_{\text{Pd}} \approx 8.5 \text{ mJ}/(\text{g atom K}^2)$,¹⁷ and $\gamma_{\text{Nb}_3\text{Sn}} \approx 13.0 \text{ mJ}/(\text{g atom K}^2)$.¹⁸ Also, disordered Nb₃Sn can have a smaller γ than Nb, and yet Nb has a T^3 dependence while Nb₃Sn still has a T^2 dependence for the resistivity. Hence we feel that this mechanism as well as the calculations for disordered alloys cannot account for the T^2 mechanism.

Until very recently it appeared that the T^2 dependence was a theoretical puzzle and the phonon frequency explanation of Webb *et al.*⁵ was an attractive solution to the problem. However, the data presented here for ordered and disordered Nb₃Sn seem to indicate that this explanation is inadequate to explain all of the data, and that one must look for other

mechanisms. Paskin¹⁹ has recently suggested that if one takes into account the strong scattering nature of the conventional electron-phonon interaction, then a T^2 mechanism can be obtained. Also a recent calculation by Halley and Imry²⁰ suggests that at low temperatures a T^2 behavior is expected for conductors with narrow electronic bands. They indicate that such a model can account for the low-temperature behavior of A15's, where narrow d bands are expected near the Fermi energy. In this context it should be mentioned that a similar T^2 behavior has been seen in another class of material with high d -band density of states, namely the high- T_c Chevrel phases.²¹

V. CONCLUSIONS

In this paper we have presented data of ordered and disordered A15 compounds and have discussed its analysis in some detail to argue that the T^2 dependence in the low-temperature resistivity of high- T_c A15 materials is an intrinsic effect. It is found that this dependence is preserved even as the material is disordered and the mean free path is reduced. Furthermore, for Mo₃Ge which has a low d -band density of states, a T^5 behavior is observed which persists to at least a $\rho(0) \sim 30 \mu\Omega \text{ cm}$. It is argued that existing theories and explanations are inadequate to consistently reproduce the observations. Recent theoretical work shows that there are refinements to present transport theories which can still yield a fundamental T^2 dependence in materials having long-range order.

It was also shown that the behavior of the coefficient A as a function of disorder could be understood within the context of the "parallel resistor" model for the saturation of resistivity. It was found that the value of ρ_{max} deduced from these measurements agrees very well with that obtained from high-temperature fits.

ACKNOWLEDGMENTS

We are grateful for discussions with many of our colleagues, including P. B. Allen, Y. Imry, J. W. Halley, and A. Paskin. This work was supported by the Department of Energy under Contract No. DE-AC02-76CH00016.

APPENDIX: DEVIATION-PLOT METHOD

There are several methods that can be used to find a power index n in the temperature dependence of the resistivity

$$\rho(T) = \rho(0) + AT^n, \quad (\text{A1})$$

such as plotting the data on log-log paper [for that one has to know $\rho(0)$ which may be difficult for materials with high T_c] or plotting resistivity versus T^n and finding the index n which produces the best straight line. However these standard methods can sometimes be misleading because it is difficult to judge graphically just how well a straight line fits the data. To provide a better way to determine the excellence of a fit we have developed a simple modification of the $\rho(T)$ vs T^n method which, with the use of a small computer, can determine the index n as precisely as the data permit. The idea of the method is the following: Suppose the resistivity is given by Eq. (A1). We want to find the true power index n for the temperature range $T_1 \leq T \leq T_2$. To do this we introduce a variable $x = T^z$ and then plot $\rho(T) = Y(x)$ as a function of x between $x_1 = T_1^z$ and $x_2 = T_2^z$. If z is equal to n , then a straight line will be obtained, whereas in all other cases another curve is obtained. Let us now connect points $Y(x_1)$ and $Y(x_2)$ with the straight line in coordinates x, y [we are using y for any ordinate, while Y is reserved for the ordinates of the resistivity curve $\rho(T)$]. We can write the equation of this straight line as

$$y(x) = Y(x_1) + \frac{Y(x_2) - Y(x_1)}{x_2 - x_1} (x - x_1) .$$

The deviation of the ordinates of the "true" curve $Y(x)$ from that of the straight line is

$$\begin{aligned} \Delta(x) &= Y(x) - y(x) \\ &= Y(x) - y(x_1) - \frac{Y(x_2) - Y(x_1)}{x_2 - x_1} (x - x_1) . \end{aligned}$$

Now we can plot the deviation $\Delta(x)$ in the interval $x_1 \leq x \leq x_2$ for different values of z . For each new value of z , the scale on the axis $x = T^z$ becomes different, but it is nevertheless convenient to keep the ends of the $\Delta(x)$ curves fixed [the ends are points $\Delta(T_1^z) = \Delta(T_2^z) = 0$], so that a bundle of curves like the ones shown on Fig. 1 will be obtained which we call a "deviation plot" (DP). Obviously, the curve closest to the x axis corresponds to the value of z closest to the true index n . If the precision of the data permits, the approximation for n can be further improved by repeating the procedure with a smaller interval in the z values. One example is shown in Fig. 7, where the described procedure is applied to Wilson's resistivity formula⁶

$$\rho_w \propto \left(\frac{T}{\Theta_D} \right)^3 \int_0^{\Theta_D/T} \frac{t^3 dt}{(e^t - 1)(1 - e^{-t})} . \quad (\text{A2})$$

(Here Θ_D is the Debye temperature.) In Fig. 7(a), z assumes values of 2, 3, and 4 and $T/\Theta_D \leq 0.09$. The index n is 3 to within ± 0.1 . A better approximation for n can be obtained from Fig. 7(b), where z assumes values of 2.9, 3.0, and 3.1. (Note that the values of Δ are amplified by a factor of 10 compared to the previous case.) From Fig. 7(b) it can be es-

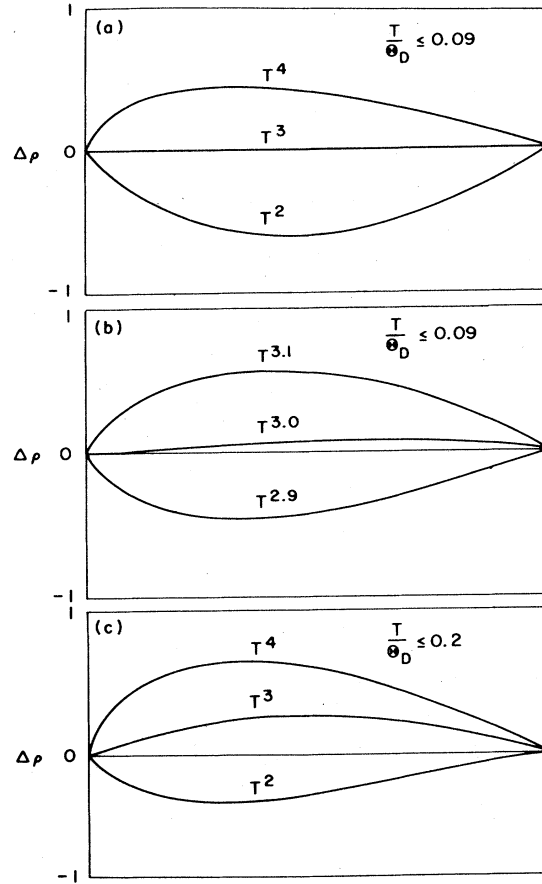


FIG. 7. Deviation-plot method applied to Wilson's resistivity formula Eq. (A2), for different temperature ranges. (a) and (b) $T/\Theta_D \leq 0.09$; (c) $T/\Theta_D \leq 0.2$.

timated that in this temperature range $n = 3 \pm 0.03$. Figure 7(c) demonstrates what happens when we choose the wider temperature range $T/\Theta_D \leq 0.2$. Now it is observed that no single power law fits the data, which is indicated by a characteristic "twisting" of all the curves. An average n decreases to a value of ~ 2.5 in accordance with the fact that at still higher temperatures Wilson's formula predicts that the resistivity will become linear in T .

To further explore the potentials of the DP method, resistivity data for commercial annealed copper wire were taken and analyzed. It is found that for Cu $n = 5 \pm 0.2$ for $T \leq 25$ K, in agreement with the Bloch-Grüneisen theory of simple metals.⁶ Data were also taken for an evaporated niobium sample with resistance ratio 10 and a T_c of 9.3 K. The DP method showed that for Nb, $n = 3 \pm 0.1$ for $T < 25$ K in agreement with Wilson's theory⁶ (Θ_D of Nb ~ 300 K, hence $T/\Theta_D < 0.085$ where the T^3 law should be valid). For higher temperatures ~ 40 K, the resistivity deviated from the T^3 behavior which agreed with Wilson's formula for $T/\Theta_D < 0.13$.

- *Present address: Bell Labs, Murray Hill, N. J. 07974.
 †Present address: Division of Neurosurgery, Medical College of Virginia, Richmond, Va. 23298.
- ¹M. Gurvitch, A. K. Ghosh, B. L. Gyorffy, H. Lutz, O. F. Kammerer, J. S. Rosner, and M. Strongin, *Phys. Rev. Lett.* **41**, 1616 (1978).
- ²H. Wiesmann, M. Gurvitch, H. Lutz, A. K. Ghosh, B. Schwartz, M. Strongin, P. B. Allen, and J. W. Halley, *Phys. Rev. Lett.* **38**, 782 (1977).
- ³D. W. Woodard and G. D. Cody, *Phys. Rev.* **136**, A166 (1964).
- ⁴S. J. Williamson and M. Milewits, in *Superconductivity in d- and f-band metals*, edited by D. H. Douglass (Plenum, New York, 1976), p. 551.
- ⁵G. W. Webb, Z. Fisk, J. J. Engelhardt, and S. D. Bader, *Phys. Rev. B* **15**, 2624 (1977).
- ⁶A. H. Wilson, *Theory of Metals* (Cambridge University Press, Cambridge, 1964).
- ⁷V. A. Marchenko, *Sov. Phys. Solid State* **15**, 1261 (1973).
- ⁸M. Gurvitch, Ph.D. dissertation (State University of New York at Stony Brook, 1978) (unpublished).
- ⁹G. S. Brown, L. R. Testardi, J. H. Wernick, A. B. Hallack, and T. H. Geballe, *Solid State Commun.* **23**, 875 (1977); see also discussion in A. K. Ghosh, M. Gurvitch, H. Wiesmann, and M. Strongin, *Phys. Rev. B* **18**, 6116 (1978).
- ¹⁰Z. Fisk and G. W. Webb, *Phys. Rev. Lett.* **36**, 1084 (1976).
- ¹¹W. L. McMillan, *Phys. Rev.* **167**, 331 (1968).
- ¹²M. Gurvitch, in *Superconductivity in d- and f-band metals* (in press).
- ¹³R. Hasegawa, *Phys. Lett. A* **36**, 425 (1971).
- ¹⁴A. I. Gubanov, *Sov. Phys. JETP* **4**, 465 (1957).
- ¹⁵P. J. Cote and B. V. Meisel, *Phys. Rev. Lett.* **39**, 102 (1977).
- ¹⁶F. J. Ohkawa, *J. Phys. Soc. Jpn.* **44**, 4 (1978).
- ¹⁷M. J. Rice, *Phys. Rev. Lett.* **25**, 1439 (1968).
- ¹⁸L. J. Vieland and A. K. Wicklund, *Phys. Rev.* **166**, 424 (1968).
- ¹⁹A. Paskin (unpublished).
- ²⁰J. W. Halley and Y. Imry (unpublished).
- ²¹J. A. Woollam and S. A. Alterovitz, *Phys. Rev. B* **19**, 749 (1979).